Stimulus-response curves of a neuronal model for noisy subthreshold oscillations and related spike generation

Martin Tobias Huber[1] and Hans Albert Braun[2]
[1]*Department of Psychiatry and Psychotherapy, University of Marburg, Rudolf-Bultmannstraße 8, D-35033 Marburg, Germany*
[2]*Institute of Normal and Pathological Physiology, University of Marburg, Deutschhausstraße 1, D-35033 Marburg, Germany*
(Received 27 September 2005; revised manuscript received 21 February 2006; published 27 April 2006)

We investigate the stimulus-dependent tuning properties of a noisy ionic conductance model for intrinsic subthreshold oscillations in membrane potential and associated spike generation. Upon depolarization by an applied current, the model exhibits subthreshold oscillatory activity with an occasional spike generation when oscillations reach the spike threshold. We consider how the amount of applied current, the noise intensity, variation of maximum conductance values, and scaling to different temperature ranges alter the responses of the model with respect to voltage traces, interspike intervals and their statistics, and the mean spike frequency curves. We demonstrate that subthreshold oscillatory neurons in the presence of noise can sensitively and also selectively be tuned by the stimulus-dependent variation of model parameters.

DOI: 10.1103/PhysRevE.73.041929 PACS number(s): 87.17.Aa, 05.45.−a, 05.40.Ca, 87.17.Nn

I. INTRODUCTION

Many neurons in the central and peripheral nervous system exhibit a characteristic electrical behavior on depolarizing stimuli. This is characterized by intrinsic subthreshold membrane potential oscillations with related action potential generation when the oscillations reach the spike threshold [1–11]. Such oscillations are an intrinsic property of the neurons and result from the interplay of different ionic conductances [3–6]. In addition, stochastic fluctuations, which are naturally present due to the inherent noisiness of neurons, play an important role for the response behavior. When oscillations operate close to the spike threshold, the noise can essentially determine whether a spike is triggered or not, and even little stochastic fluctuations can initiate action potential generation [8,12–18].

The role of subthreshold oscillations for neuronal function is different depending on location and function of the involved neuron. That is, a peripheral neuron or sensory receptor responsible for sensing environmental sensory stimuli can use stimulus-dependent modulations of subthreshold oscillations for that purpose [8]. Probably the most interesting example for such encoding with oscillations and noise are shark electroreceptors. These receptors can encode electrical and thermal stimuli, and it was demonstrated experimentally that these electroreceptors do use intrinsic subthreshold membrane potential oscillations in cooperation with stochastic fluctuations to improve their encoding sensitivity to these stimuli. Moreover, selective stimulus-dependent modulation of the spiking probability per oscillation cycle and oscillation frequency is used for the differential encoding of the two sensory modalities [8]. This is because electrical stimuli rather selectively modulate the spiking probability, whereas temperature alters both the spiking probability and the frequency. Such temperature-dependent effects on neuronal oscillations are also known from temperature encoding by peripheral thermoreceptors [12,13,16,19,20].

Neurons located in central structures, such as the entorhinal cortex [6] or amygdala [4,5], are supposed to use the oscillations for the timing of collective rhythmic behaviors, e.g., the limbic theta rhythm and the generation of synchronized responses [2,3,21–24]. Fine tuning of oscillatory responses by neuromodulatory substances, e.g., due to cholinergic and dopaminergic alteration of oscillatory dynamics, were described [25,26] and could also be used for the proper adjustment of signal encoding properties in the central nervous system. The importance of noise for subthreshold oscillations was considered also with regard to central neurons [18,27].

However, subthreshold oscillations can also become important under pathological conditions. This is the case with pain-sensitive (nociceptive) dorsal root ganglion neurons (peripheral sensory neurons). In such nociceptive neurons, previous nerve injury enhances subthreshold oscillatory activity and increases the number of subthreshold oscillatory cells. These subthreshold oscillations seem necessary for sustained spiking and ectopic spike discharge, and hence the development of neuropathic pain states [7,9,10,28–32]. Interestingly, spike patterns and interspike interval histograms (ISIHs) recorded from such injured sensory neurons [10] resemble the ones recorded from shark electroreceptors and subthreshold oscillating thermoreceptors, again indicating a significant influence of stochastic fluctuations on oscillatory responses [8]. The productive role of stochastic fluctuations and specifically stochastic resonance for sensory encoding and biological systems in general has attracted much attention since the first paper on stochastic resonance in a sensory receptor was published by Moss and co-workers [33]. Up until now, a multitude of work addressed the role of noise in biological systems and studies include the molecular, cellular, systems, and even behavioral level [8,12,18,33–56]. In addition, recent experimental studies have begun to emphasize the role of random synaptic background activity for the modulation of neuronal sensitivity and gain control in cortical neurons [57–59], and very recently noise-dependent linearization of spike-burst transitions in thalamic neurons could be demonstrated experimentally [60].

The effect of tuning of noisy subthreshold oscillations by the alteration of ionic conductance parameters and the result-

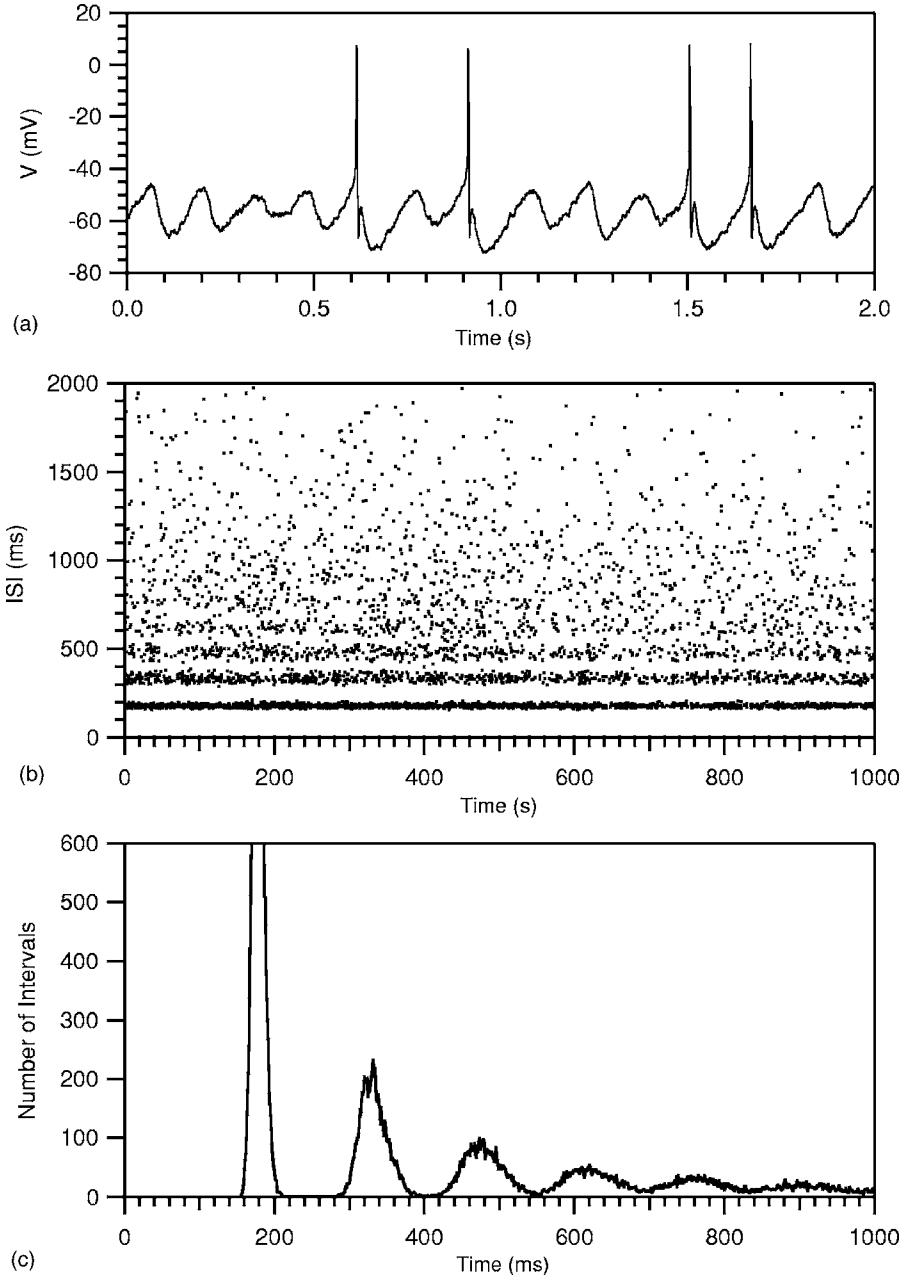

FIG. 1. Noisy subthreshold oscillations and related spike generation generated by the model. (a) Time sequence of the membrane voltage, (b) time plot of successive interspike intervals from a longer simulation run, and (c) the corresponding ISIH. Simulation time $t=1000$ s, $I_{app}=1.3$ mA/cm^2, noise intensity $D=0.1$.

ing effects on signal encoding and neuromodulation have attracted less interest, perhaps with the exception of impulse pattern modifications in peripheral thermoreceptors [12,16,19]. The situation, however, is different from stochastic resonance effects due to the modulation of the noise intensity, and it is different from the gain modulation and sensitivity adjustment by noise-dependent linearization of stimulus-response curves. In our case, the tuning is caused by the intrinsic parameters of the oscillations. The noise is needed to get smooth, continuous, and more linear stimulus-response curves, but the actual noise intensity is not of critical importance. We note in passing that we gave a brief report on stochastic resonance effects in an almost identical model [56]. For a thorough account of stochastic resonance in different types of oscillatory neurons, see the paper by Longtin [61].

For the reasons given above, we concentrate in the present paper on response behaviors and tuning curves resulting from modulation of neuronal oscillations in the presence of a fixed noise level. We use a computational approach and consider the modulatory features of a minimal, yet physiologically plausible, ionic conductance model for noisy subthreshold oscillations and associated spiking, which is able to reproduce some of the essential encoding and modulatory properties observed experimentally. The paper is organized as follows. We start with the situation where the depolarizing electrical current application leads to noisy subthreshold oscillations and action potentials in our model neuron, and demonstrate the characteristic voltage traces, interspike interval plots, and interspike interval histograms. In the following sections, we then investigate systematically how the variation of the applied current I_{app}, the noise intensity D, the

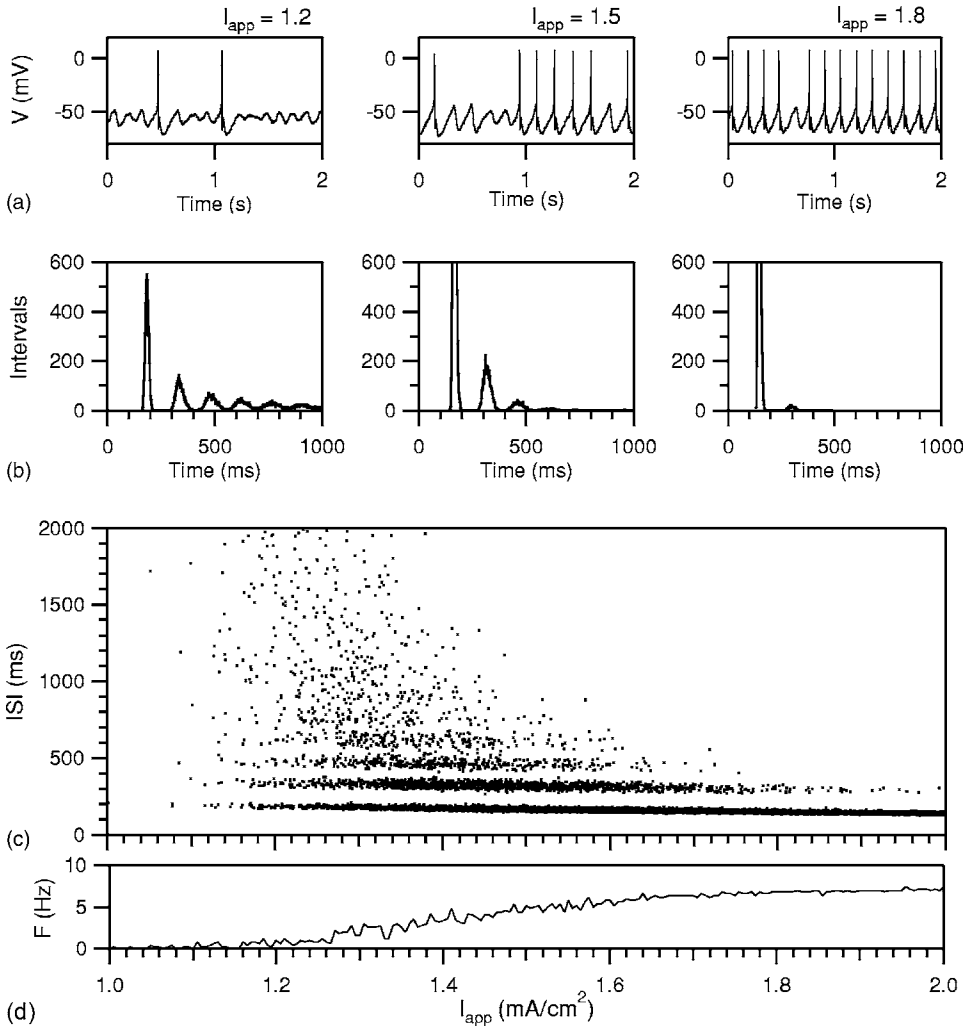

FIG. 2. Effect of depolarizing applied current I_{app}. (a) Voltage traces and (b) ISIHs for $I_{app}=1.2$, 1.5, and 1.8 mA/cm^2, (c) time plot of successive ISIs and (d) mean spike frequency (F) in response to a ramp-shaped change of the applied current (time=5000 s, increment $\Delta I_{app}=0.0002$ mA cm^{-2} ms^{-1}, noise intensity $D=0.1$).

subthreshold potassium conductance g_{Ks}, and the temperature T change the model neuron's responses with respect to voltage traces, interspike intervals (ISIs), ISIHs and corresponding mean spike frequency curves. We end with a short summary and concluding remarks.

II. MODEL

A. Physiological background

Our model is designed to account for a specific type of neuronal impulse generation which—as described above—is a mixture of subthreshold membrane potential oscillations and associated spike generation. In experimental recordings, this behavior appears as a periodic spiking interrupted by random skipping of spikes at integer multiples of a basic oscillation period, which leads to characteristic multimodal interspike interval histograms (a typical example is shown in Fig. 1). It is reasonable to assume and partly known that different ionic mechanisms can generate this behavior as it can be seen in a diversity of neurons in specific situations (e.g., cold receptors at high temperatures), and as it is found in very different regions and systems of the brain and in very different biological species, such as mammals or shark electroreceptors (e.g. [1–8]). Remarkably, at least some of these neurons operate with rather simple sets of ionic conductances, i.e., a persistent sodium conductance and a subthreshold potassium conductance. For example, neither the neurons in the entorhinal cortex nor shark electroreceptors seem to need calcium dynamics, e.g., calcium-dependent potassium conductances, which are a major component in many other neurons with neuronal oscillations—especially for slow-wave bursters (see e.g., [13,16] and literature therein for the work of many other authors).

It is the aim of this study to evaluate what encoding properties can be achieved in the presence of noise with such a minimal set of ionic conductances. As an emphasis is placed on ionic conductances, we do not consider reduced models, such as integrate-and-fire models or FitzHugh-Nagumo models [62], but use the classical Hodgkin-Huxley-type approach—although in a simplified version—with explicit relations to specific ion currents as they can be recorded experimentally. Simplifications in comparison to other existing HH-type models are, particularly with respect to the typical HH-like action potential conductances (instantaneous activation of the fast sodium conductance, no inactivation of conductances), as not the precise representation of the action potentials themselves but the temporal patterns of impulse generation and their modulation are of major interest in this study. We also have eliminated all exponents for the activa-

tion variables, which is a further simplification of a previous version of the model [39,56]. The resulting minimal ionic model can realistically represent noisy subthreshold oscillations and related spiking when compared to the experimental data as well to models using a more detailed HH-formalism [18,24]. A similar simplification approach was used by us with respect to calcium-dependent oscillations and bursting in cold receptors, e.g. [19] compared to [16].

B. Ionic conductances

Our model consists of two sets of simplified sodium and potassium conductances operating at two different membrane potentials and two different time scales: A conventional Hodgkin/Huxley-type spike encoder is represented by rapid high-voltage activating g_{Na} and g_{K}. Also, subthreshold oscillations are modeled here as only voltage-dependent conductances, which are—according to data from the entorhinal cortex [6]—a persistent sodium conductance, g_{Nap}, and a subthreshold potassium conductance, g_{Ks}. With an additional term for external current application and noise, this gives the following membrane equation:

$$C_M dV/dt = -I_1 - I_{\mathrm{Nap}} - I_{\mathrm{Ks}} - I_{\mathrm{Na}} - I_{\mathrm{K}} + I_{\mathrm{app}} + \zeta, \qquad (1)$$

where $C_M = 1\ \mu\mathrm{F/cm^2}$ is the membrane capacity, V is the membrane voltage, $I_1 = g_1\ (V - V_1)$ is a leak current with $g_1 = 0.1\ \mathrm{mS/cm^2}$, and $V_1 = -60$ mV. I_{app} is the injected current and ζ is the Gaussian white noise with the properties $\langle \zeta(t) = 0 \rangle$ and $\langle \zeta(t)\zeta(s) \rangle = 2D\delta(t-s)$, which determines all of its statistical features.

The voltage-dependent currents I_{Nap}, I_{Ks}, I_{Na}, and I_{K} are modeled as

$$I_i = \rho g_i a_i (V - V_i), \qquad (2)$$

where ρ is a temperaturelike scaling factor, g_i are the respective maximum conductances (i denotes Na, Nap, K, Ks), a_i are the voltage-dependent activation variables, V is the membrane potential, and V_i is the respective Nernst potential. The activation variables are given as

$$da_i/dt = \varphi(F_i - a_i)/\tau_i \qquad (3)$$

with

$$F_i = 1/\{1 + \exp[-s_i(V - V_{0,i})]\}, \qquad (4)$$

where φ is a temperaturelike scaling factor, τ_i are time constants, s_i is the slope, and $V_{0,i}$ is the half-activation potential. Activation of I_{Na} is instantaneous, thus $a_{\mathrm{Na}} = a_{\mathrm{Na}\infty}$. The temperaturelike scaling factors ρ (for ionic currents) and φ (for ionic kinetics) are given as $\varphi = 3.0^{(T-25)/10}$ and $\rho = 1.3^{(T-25)/10}$ with T as the temperature in °C [63].

C. Stochastic influences in the model

Membrane noise consists of thermal noise, conductance noise including synaptic noise, and electrogenic pump noise. The situation is complicated as in experimental impulse recordings of sensory receptors; the different noise sources cannot be distinguished so far and any specific noise realization at the current state of physiological knowledge is therefore purely arbitrarily. However, we can take advantage of the fact that the specific noise origin seems to be of minor relevance, at least for the purpose of this study, which focuses on a particular impulse pattern. These patterns, indeed, can be achieved with quite different noise realizations—provided the appropriate dynamics with subthreshold oscillations. At the level of impulse patterns and tuning curves, which we consider here, qualitatively identical responses can be obtained with quite different noise implementations as we recently demonstrated by an orientating comparative analysis of the effects of current noise and conductance noise [64]. Accordingly, we followed the discussion and approach given by Longtin and Hinzer [16] and used a simple white-noise term in the membrane equation, which includes the different noise sources as a first approximation.

The system of equations was solved numerically by the use of the forward Euler integration method with a step size adjusted to 0.1 ms. The white noise was generated with the Box-Mueller algorithm and implemented in the Euler version

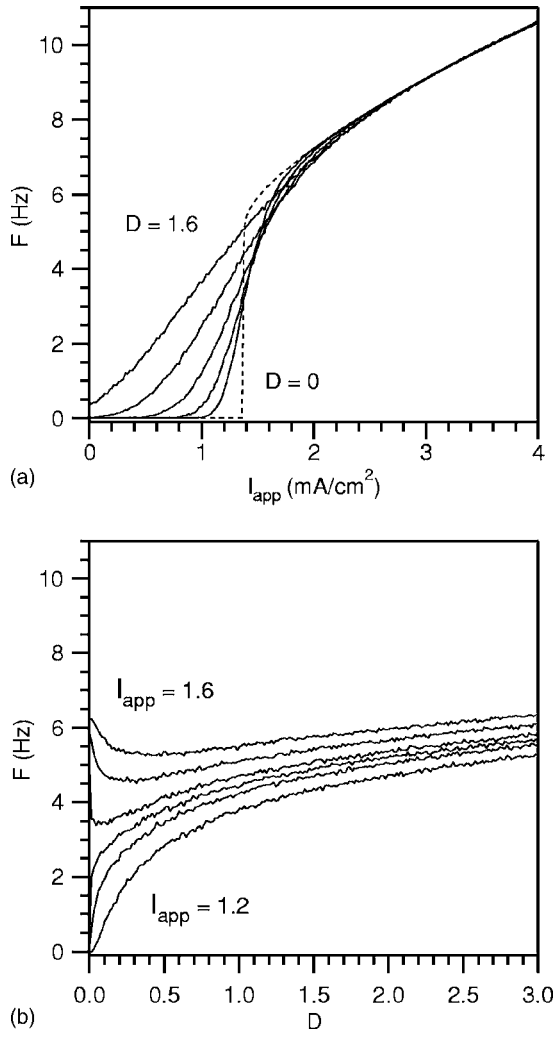

FIG. 3. (a) Mean spike frequency F (Hz) versus I_{app} ($\mathrm{mA/cm^2}$) for different values of the noise intensity ($D = 0$, 0.1, 0.2, 0.4, 0.8, and 1.6). (b) Mean spike frequency F versus D for different values of the applied current ($I_{\mathrm{app}} = 1.2$, 1.3, 1.35, 1.4, 1.5, and 1.6 $\mathrm{mA/cm^2}$).

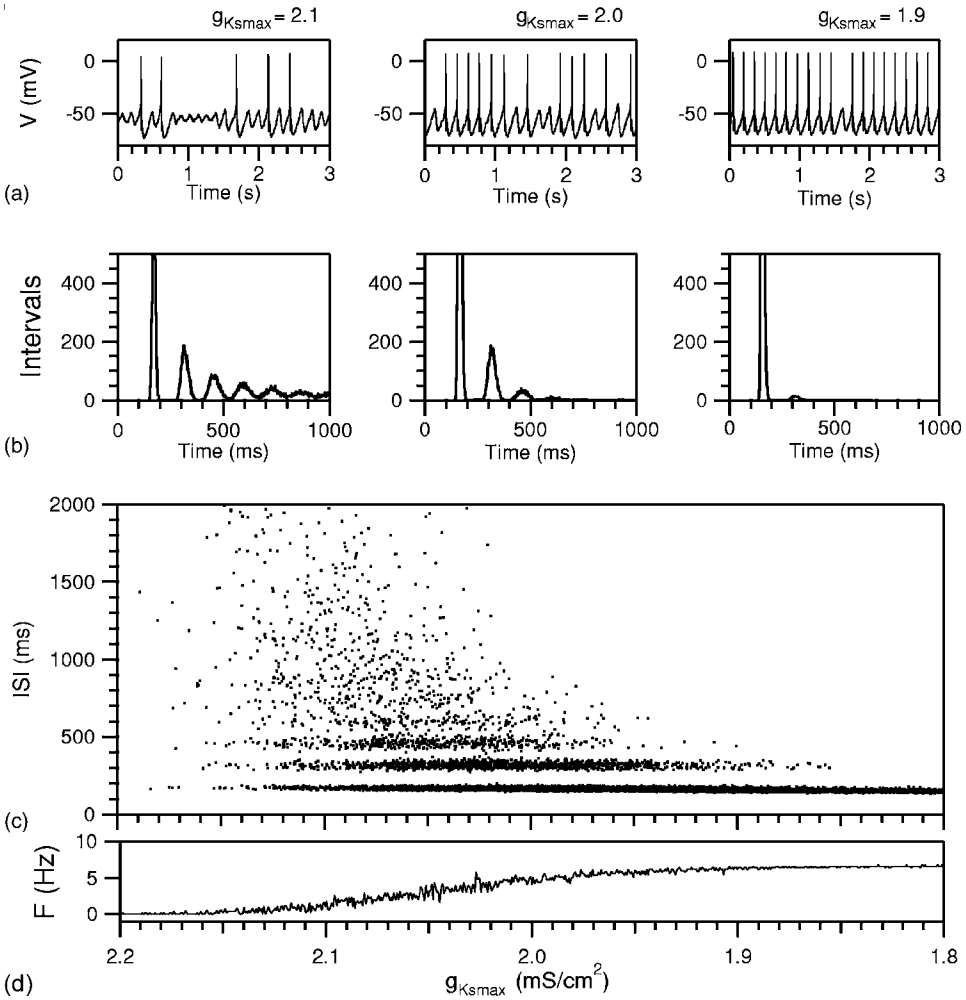

FIG. 4. Effect of potassium conductance g_{Ks}. (a) Voltage traces and (b) ISIHs for $g_{Ksmax}=2.1$, 2.0, and 1.9 mS/cm^2, (c) time plot of successive ISIs, and (d) mean spike frequency (F) in response to a ramp-shaped change of g_{Ksmax} (time=5000 s, $\Delta g_{Ksmax}=8\times10^{-5}$ mS cm^{-2} ms^{-1}, noise intensity $D=0.1$, $I_{app}=1.5$ mA/cm^2).

of the integration as described in Fox *et al.* [65]. Numerical parameter values: $V_{Na}=50$, $V_K=-90$, $g_{Na}=2.0$, $g_K=2.0$, $g_{Nap}=0.4$, $g_{Ks}=2.0$, $s_{Na}=s_K=s_{Nap}=s_{Ks}=0.25$, $\tau_K=2.0$, $\tau_{Nap}=10$, $\tau_{Ks}=50$, $V_{0Na}=V_{0K}=-25$, and $V_{Nap}=V_{0Ks}=-40$. The units of measure are in ms, mV, mS/cm^2, and mA/cm^2.

III. RESULTS

Our starting point is the model depolarized by an applied current I_{app} which results in subthreshold oscillations of the membrane potential (Fig. 1). In this situation, noise becomes important for spike generation because it essentially determines whether or not a spike is triggered. Without noise, the model would remain completely subthreshold in the simulations shown in Fig. 1. With noise, we observe a characteristic response pattern characterized by subthreshold oscillations, and oscillations that occasionally trigger action potentials. In the plot of successive interspike intervals, this behavior is reflected by separated bands of intervals [Fig. 1(b)]. The ISIH shows the well-known multimodal interval distribution with interval peaks located at approximate integer multiples of a basic oscillation period [Fig. 1(c)].

The amplitude of the oscillations and hence the likelihood for spike generation depend on the level of depolarizing current I_{app} (Fig. 2). At low levels of I_{app}, a spike is triggered only rarely whereas on higher levels of I_{app} an oscillation only occasionally fails to trigger a spike [Fig. 2(a)]. Accordingly, in the ISIHs, the first interval peak representing the basic oscillation period increases with increasing depolarization and the multimodality decreases [Fig. 2(b)]. The continuous ramplike change of I_{app} and its effect on the oscillatory responses are demonstrated in the time plot of interspike intervals [Fig. 2(c)]. First, intervals are scattered to long durations and are more or less triggered randomly by the noise. In intermediate ranges, distinctive bands of intervals occur resulting from the depolarization-induced oscillations and associated periodic spike generation. Finally, when almost all oscillations reach spike threshold, the intervals become concentrated on the band which represents the basic oscillation period.

In the whole range from occasional spikes to fully periodic spiking, the oscillation frequency is not much affected. This is indicated by an almost unchanged location of the interspike interval peaks and bands, respectively [Figs. 2(b) and 2(c)]. The reason is that the model operates close to the spike threshold where small changes in membrane depolarization have significant effects on the probability of spike generation without similar pronounced effects on the oscillation frequency. This effect is also reflected in the averaged measure of the mean spike frequency curve. In the mean spike frequency (F) versus applied current (I_{app}) plot, this is

the range where the increase in F is most pronounced [Fig. 3(a)] and, where under fully deterministic conditions [$D=0$; dashed curve in Fig. 3(a)], F jumps in a steplike way when I_{app} crosses a threshold value ($I_{app} > 1.34$ mA/cm^2 in our model). The noise smoothes the steplike nonlinearity of the deterministic curve. Increasing the noise intensity reduces the slope and, in this way, linearizes the relation. The response range increases in that way, however, at the cost of the response sensitivity. Figure 3(a) also shows that increasing the depolarizing current monotonically also increases the spike frequency in the suprathreshold response range. The increase of F in the suprathreshold range now results from an I_{app}-induced acceleration of the oscillation frequency and not from modulation of the spiking probability as is the case in the range close to the spike threshold.

The effect of the noise intensity on the mean spiking frequency for different fixed values of I_{app} is shown in Fig. 3(b). Two principally different behaviors are observed depending on whether the model is in a subthreshold or suprathreshold state. In the subthreshold range, F rises monotonically with the noise intensity. Here, the noise can initiate spike generation in otherwise subthreshold oscillations, and F rises as higher noise intensities lead to a higher spiking probability. In the suprathreshold range, the situation is different as F initially decreases with increasing noise intensity and increases again with higher levels of noise. In the suprathreshold situation, some noise can suppress the spiking in former spike-triggering oscillations. However, with high noise levels, the excitatory effect of the noise becomes dominant and, accordingly, F rises monotonically. In both cases, the initial increase or decrease in the mean frequency is most pronounced at low-to-moderate noise intensities, where the noise interacts with the oscillatory dynamics [Fig. 3(b)]. High noise intensities then overwhelm the dynamics, destroy the oscillations, and spiking is no longer related to an underlying periodic process.

We next consider the modulatory effect of ionic conductances underlying the subthreshold oscillations. As an example, we chose the subthreshold potassium conductance g_{Ks} and vary the maximum conductance g_{Ksmax}. Experimentally, this would correspond to the application of potassium channel blockers, such as 4-aminopyridine or, physiologically, to the action of channel-blocking neuromodulatory substances. Figure 4 shows the change of interspike intervals and the mean spike frequency in response to a ramplike change of g_{Ksmax} [Figs. 4(c) and 4(d)] together with voltage traces and ISIHs at three different values of g_{Ksmax} [Figs. 4(a) and 4(b)]. A reduction of the g_{Ksmax} has a depolarizing effect on the membrane voltage. In turn, subthreshold oscillations develop ($g_{Ksmax}=2.1$ mS/cm^2) leading to the characteristic multimodality of the ISIHs and interspike interval plots. By further decreasing g_{Ksmax}, the subthreshold oscillations rise in amplitude until finally periodic spiking occurs. Correspondingly, the ISIHs and interspike plots change to unimodal distributions ($g_{Ksmax}=2.0->1.9$ mS/cm^2).

The mean spiking frequency F increases monotonically and approximately sigmoidal with decreasing g_{Ksmax} values [Figs. 4(d) and 5(a)]. The response range then can be tuned to lower or higher g_{Ksmax} values by respective adjustment of the amount of I_{app}, that is by adjusting the preactivation level

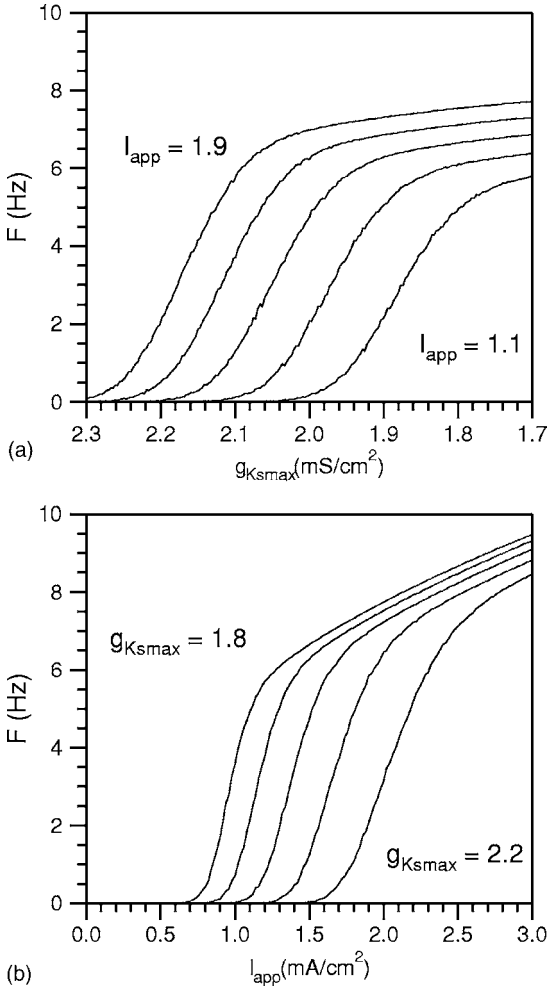

FIG. 5. (a) Mean spike frequency F (Hz) versus g_{Ksmax} (mS/cm^2) for different values of applied current ($I_{app}=1.1$, 1.3, 1.5, 1.7, and 1.9 mA/cm^2). (b) Mean spike frequency F (Hz) versus I_{app} (mA/cm^2) for different values of g_{Ksmax} (1.8, 1.9, 2.0, 2.1, and 2.2 mS/cm^2).

with I_{app} [Fig. 5(a)]. Higher values of I_{app} shift the F curve to higher g_{Ksmax} values and vice versa. Similarly, the mean spiking frequency, dependent upon I_{app} can be tuned to lower or higher values by adjusting the g_{Ksmax}, that is by adjusting the preactivation level with the g_{Ks} [Fig. 5(b)]. Reducing the g_{Ksmax} decreases the total amount of repolarizing ionic current, and for this reason less applied current is needed for membrane depolarization. Accordingly, the F curve is shifted to lower I_{app} values. Increasing the g_{Ksmax} has the opposite effect, because it increases the repolarizing ionic current and therefore the amount of I_{app} needed for depolarization.

The last part of the results considers how temperature scaling of the ionic conductances alters the responses of the model. Voltage traces and ISIHs at three different steady temperatures are shown in Figs. 6(a) and 6(b). A time plot of the interspike intervals in response to a ramplike temperature change and the corresponding mean spiking frequency is demonstrated in Fig. 6(b). Temperature scaling predominantly alters the time constants τ_i of the ionic currents and, to a minor degree, the values of the maximum ionic currents [see Eqs. (2) and (3) in Sec. II]. The temperature effect on

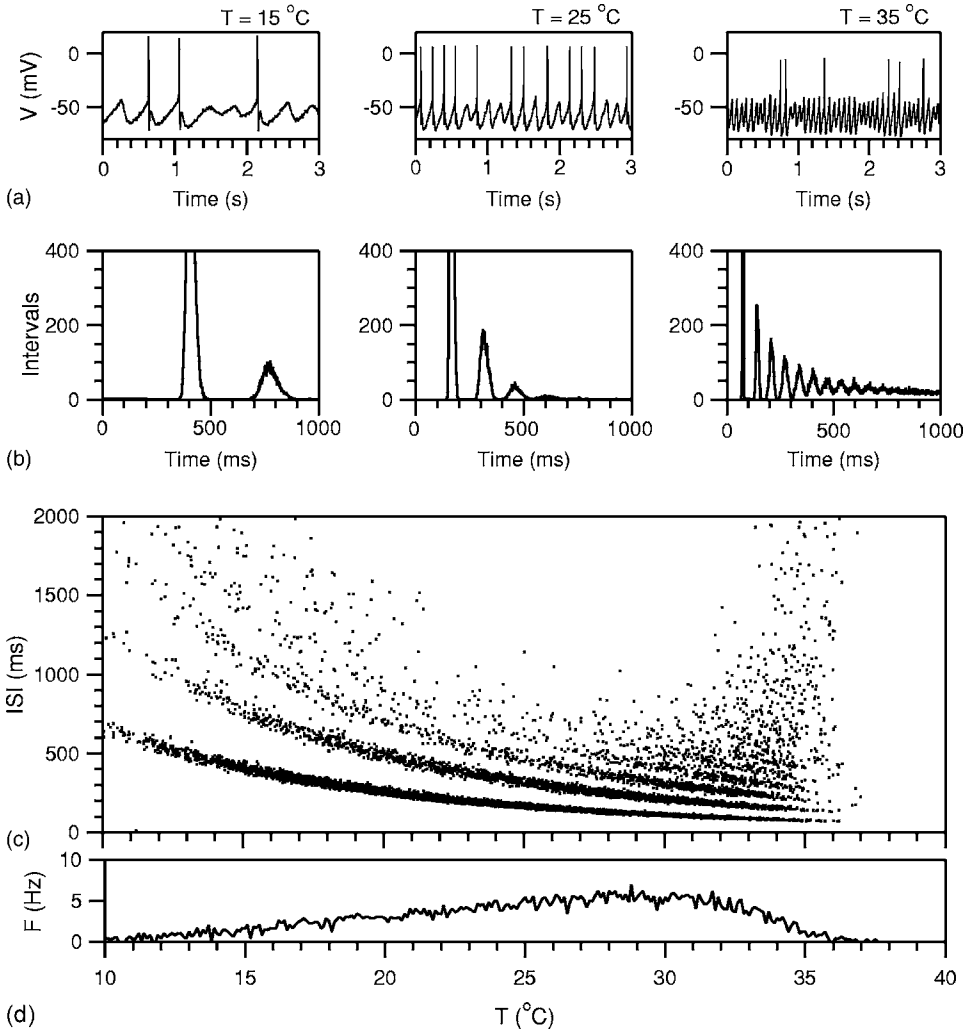

FIG. 6. Effect of temperature. (a) Voltage traces and (b) ISIHs for $T=15$, 25, and 35 °C, (c) time plot of successive ISIs, and (d) mean spike frequency (F) in response to a ramp-shaped change of T (time = 5000 s, increment $\Delta T=0.006$ °C/ms, noise intensity $D=0.1$, and $I_{app}=1.5$ mA/cm^2).

the activation time constants in turn has a pronounced influence on the frequency of the subthreshold oscillations and action potentials [Fig. 6(a)]. The effects on amplitudes of oscillations and action potentials are to some extent compensated for by the changes of the maximum ionic currents, which decrease with decreasing T and vice versa. The dominant effect on the oscillation frequency leads to characteristic changes in the ISIHs and an ISI plot [Figs. 6(b) and 6(c)]. The acceleration of the oscillation frequency with rising temperature increases the number of subthreshold oscillations. This is because oscillations then become too fast to initiate action potentials during an oscillation cycle [Figs. 6(a) and 6(b)]. In the ISI time plot, the bands of intervals successively change to shorter interval durations and, with high temperatures, a scattering to longer interval durations occurs. The latter results from the accelerating oscillations, which more and more fail to trigger spikes [Fig. 6(c)].

The acceleration of the oscillation frequency with associated changes in the spiking probability has a characteristic effect on the mean frequency curve, which is very different from the stimulus-response relations obtained by the variation of I_{app} or g_{Ksmax}. In the case of temperature variation, $F(T)$ first rises with increasing temperature, but then passes through a maximum and declines again on further increasing T [Figs. 6(d) and 7(a)]. The rise in F is due to the increase in the oscillation frequency, and which in turn results from temperature-accelerated ionic kinetics. The following decrease in F results from the increasing number of faster and faster subthreshold oscillations, which successively fail to trigger spikes. The maximum value of F, as well as the slope and response range of the $F(T)$ curve, also depends on the level of depolarizing current I_{app} [Fig. 7(a)]. When the model neuron is in a more depolarized state, oscillatory activity is more pronounced and suprathreshold. In this case, oscillations can become much faster (and F much higher) until they fail to trigger spikes when becoming subthreshold (e.g., $I_{app}=2.5$ mA/cm^2 versus $I_{app}=1.3$ mA/cm^2). It should be noted that noise enlarges the response range with respect to T as noise can induce spiking in subthreshold oscillations. Without noise, $F(T)$ would rise monotonically up to a certain limit and then would immediately drop to zero when oscillations become subthreshold.

The corresponding F versus I_{app} curves at different fixed temperature levels also reflect the temperature-dependent variation of the oscillation frequency and associated spiking probability per oscillation cycle [Fig. 7(b)]. The F-I_{app} curves increase monotonically with increasing I_{app}. The obtainable maximum frequencies depend on the applied temperature range, and higher F values are achievable with higher temperatures. However, high-temperature levels need higher lev-

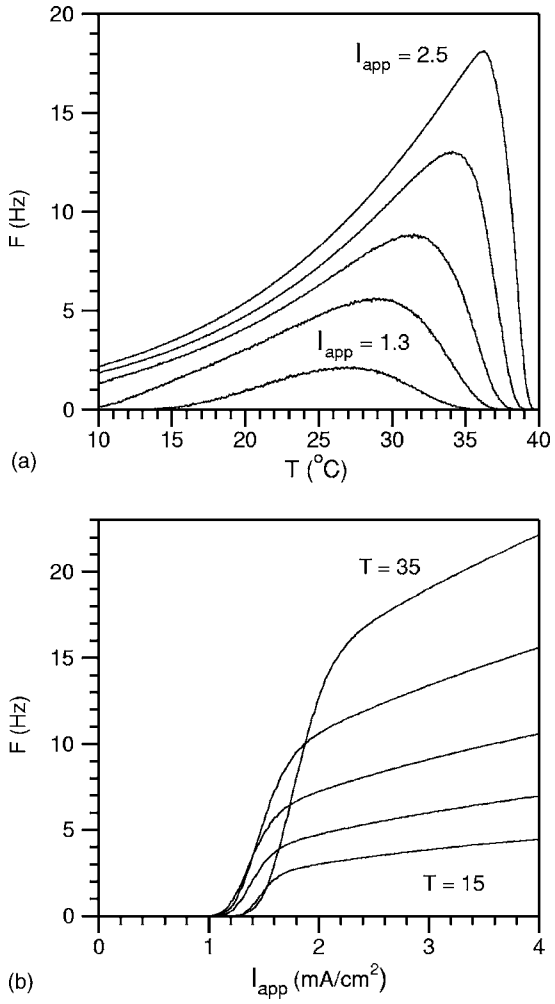

FIG. 7. (a) Mean spike frequency F (Hz) versus temperature T (°C) for different values of applied current (I_{app}=1.3, 1.5, 1.7, 2.0, and 2.5 mA/cm^2). (b) Mean spike frequency F (Hz) versus I_{app} (mA/cm^2) for different values of the temperature (T=15, 20, 25, 30, and 35 °C).

els of depolarization (larger I_{app}) because of the very short suprathreshold periods of the fast oscillations [Fig. 7(b): T =35 °C]. Further increases in I_{app} in the high-temperature range then result in a steep increase of the mean spike frequency, which is much steeper than the ones obtained at lower temperature ranges. These results demonstrate that the temperature-dependent modulation of noisy oscillations (i.e., oscillation frequency and spiking probability) has pronounced effects on temporal response patterns (voltage traces, ISIs, and ISIHs) as well as on the mean spike frequency curve and its respective slope (or gain).

IV. SUMMARY AND CONCLUSIONS

Our results presented here demonstrate that a minimal ionic conductance model for noisy subthreshold oscillations and related spike generation exhibits interesting modulatory features on physiologically relevant parameter variations. Modulatory effects thereby occur in the temporal response patterns (voltage traces and ISI distributions) as well as when the mean spike frequency is considered as a measure for signal or stimulus encoding. All of the described effects were obtained by modulation of *deterministic* parameter values (i.e., I_{app}, g_{Ksmax}, or the temperature scaling coefficients) which resulted in the variation of the oscillation frequencies and amplitudes and associated changes in the spiking probability per oscillation cycle.

The full range of responses is thereby only possible because the model includes noise. This is because only the modulation of noise-induced transitions from subthreshold oscillations to spike-triggering oscillations allows for the pronounced changes in responses, even on small parameter changes demonstrated by the changes in spike frequency and ISI statistics. However, although noise is an essential ingredient, the observed modulatory effects resulting from the modulation of applied current, ionic conductance levels, or temperature scaling are not critically dependent on the actual noise intensity. That is, similar tuning behaviors are obtained at very different noise intensities indicating the robustness of the observed behaviors. In addition to this, a variety of modulatory effects can be expected from tuning the noise intensity, such as stochastic or coherence resonance effects, and linearization of responses pointing to even more potential modulatory capabilities resulting from the interplay of oscillations and noise (see, e.g., [66–69]). One such modulatory effect is gain control (change of the slope of the response curve) by synaptic background activity ("synaptic noise") which in recent years has attracted much attention in modeling [57] and experimental [58–60] studies of cortical neurons. Although our study was not intended to account for the complex mechanisms involved in altered synaptic activity and our simulations with altered noise intensity were more intended to show the robustness of the response curves with respect to noise, it is notable that even the simple model with white noise can account quite well for some of the experimental findings (see e.g., Fig. 1 in [60]). A further elucidation of the basic biophysical principles underlying such gain modulation should therefore be of interest.

Many studies have addressed the importance of noise and, in particular, noise tuning in neurons and neuronal models, and some studies have also addressed deterministic subthreshold oscillations [3,18,24]. Our study shows that the tuning of the oscillations themselves or, more correctly, the deterministic parameters underlying the oscillatory responses, plays an equally important role for the overall encoding and modulatory properties. In addition, the effects demonstrated for a simple ionic conductance model have their real counterparts in biology. The deterministic parameters have a clear physiological meaning, such as, e.g., neuromodulation of a potassium conductance in a central nervous system neuron [25,70], encoding of environmental electrical or thermal stimuli by a sensory receptor neuron [8], or the pathophysiological relevant oscillatory response of dorsal root ganglion cells to nerve injury resulting from changed ionic conductance balances [7,9,29].

So far, dorsal root ganglion cells are the best example for a pathophysiological relevance of noisy subthreshold oscillations, and shark electroreceptors are the best example for the direct and differential encoding of sensory stimuli using this mechanism. In both cases, the interplay of oscillations and

noise provides for a large sensitivity, and in the case of the electroreceptor also for differential encoding of electrical and thermal sensory stimuli by selective modulation of the noisy oscillations. Although several differences exist between cortical neurons, dorsal root ganglion cells, and sensory receptors including the respective specific biological equipment, our study shows that some of the relevant behaviors can be represented with a simplified and generalized ionic conductance model. Being inherently noisy and tentatively oscillatory due to their nonlinearity, it seems that neurons have learned to use the two features for neuromodulation and signal encoding under physiological and pathophysiological conditions. Our study here is limited to neuromodulation and stimulus encoding at the single neuron level. We suggest that future studies should also consider the described effects with respect to coupled neurons and larger-scale neuronal networks.

ACKNOWLEDGMENT

We thank Lutz Schimansky-Geier for most valuable discussions and help with noise and nonlinear dynamics. Supported by an research grant of the EU Network of Excellence No. E005137 BioSim.

[1] R. Llinas and Y. Yarom, J. Physiol. (London) **376**, 163 (1986).
[2] D. Desmaisons, J. D. Vincent, and P. M. Lledo, J. Neurosci. **19**, 10727 (1999).
[3] Y. Gutfreund, Y. Yarom, and I. Segev, J. Physiol. (London) **483**, 621 (1995).
[4] D. Pare, H. C. Pape, and J. Dong, J. Neurophysiol. **74**, 1179 (1995).
[5] H. C. Pape, D. Pare, and R. B. Driesgang, J. Neurophysiol. **79**, 205 (1998).
[6] A. Alonso and K. Klink, J. Neurophysiol. **70**, 128 (1993).
[7] R. Amir, M. Michaelis, and M. Devor, J. Neurosci. **19**, 8589 (1999).
[8] H. A. Braun, H. Wissing, K. Schäfer, and M. C. Hirsch, Nature (London) **367**, 270 (1994).
[9] J. L. Xing, S. J. Hu, and K. P. Long, Brain Res. **901**, 128 (2001).
[10] J. L. Xing, S. J. Hu, H. Xu, S. Han, and Y. H. Wan, NeuroReport **12**, 1311 (2001).
[11] D. Schmitz, T. Gloveli, J. Behr, T. Dugladze, and U. Heinemann, Neuroscience **85**, 999 (1998).
[12] H. A. Braun, H. Bade, and H. Hensel, Pfluegers Arch. **386**, 1 (1980).
[13] H. A. Braun *et al.*, Int. J. Bifurcation Chaos Appl. Sci. Eng. **8**, 881 (1998).
[14] H. A. Braun, K. Voigt, and M. T. Huber, BioSystems **71**, 39 (2003).
[15] A. Longtin, A. Bulsara, and F. Moss, Phys. Rev. Lett. **67**, 656 (1991).
[16] A. Longtin and K. Hinzer, Neural Comput. **8**, 215 (1995).
[17] J. A. White, J. T. Rubinstein, and A. R. Kay, Trends Neurosci. **23**, 131 (2000).
[18] J. A. White, R. Klink, A. Alonso, and A. R. Kay, J. Neurophysiol. **80**, 262 (1998).
[19] H. A. Braun, K. Schäfer, K. Voigt, and M. T. Huber, Nova Acta Leopold. **88**, 293 (2003).
[20] M. T. Huber *et al.*, Chaos, Solitons Fractals **11**, 1896 (2000).
[21] I. Lampl and Y. Yarom, J. Neurophysiol. **70**, 2181 (1993).
[22] B. Hutcheon and Y. Yarom, Trends Neurosci. **23**, 216 (2000).
[23] A. K. Engel, P. Fries, and W. Singer, Nat. Rev. Neurosci. **2**, 704 (2001).
[24] X. J. Wang, NeuroReport **5**, 221 (1993).
[25] R. Klink and A. Alonso, J. Neurophysiol. **77**, 1813 (1997).
[26] E. Geijo-Barrientos and C. Pastore, Eur. J. Neurosci. **7**, 358 (1995).
[27] I. Erchova, G. Kreck, U. Heinemann, and A. V. M. Herz, J. Physiol. (London) **560**, 89 (2004).
[28] R. Amir, M. Michaelis, and M. Devor, J. Neurosci. **22**, 1187 (2002).
[29] R. Amir, C. N. Liu, J. K. Kocsis, and M. Devor, Brain **125**, 421 (2002).
[30] R. Amir, J. D. Kocsis, and M. Devor, J. Neurosci. **25**, 2576 (2005).
[31] C. N. Liu, M. Michaelis, R. Amir, and M. Devor, J. Neurophysiol. **84**, 205 (2000).
[32] C. N. Liu, M. Devor, S. G. Waxman, and J. D. Kocsis, J. Neurophysiol. **87**, 2009 (2002).
[33] J. K. Douglass, L. Wilkens, E. Pantazelou, and F. Moss, Nature (London) **365**, 337 (1993).
[34] T. S. Gardner, C. R. Cantor, and J. J. Collins, Nature (London) **403**, 339 (2000).
[35] J. Hasty, J. Pradines, M. Dolnik, and J. J. Collins, Proc. Natl. Acad. Sci. U.S.A. **97**, 2075 (2000).
[36] S. M. Bezrukov and I. Vodyanoy, Nature (London) **378**, 362 (1995).
[37] R. D. Astumian, R. K. Adair, and J. C. Weaver, Nature (London) **388**, 632 (1997).
[38] D. Petracchi *et al.*, Biophys. J. **66**, 1844 (1994).
[39] M. T. Huber *et al.*, BioSystems **48**, 95 (1998).
[40] A. Longtin, J. Stat. Phys. **70**, 309 (1993).
[41] J. E. Levin and J. P. Miller, Nature (London) **380**, 165 (1996).
[42] B. J. Gluckman, T. I. Netoff, E. J. Neel, W. L. Ditto, M. L. Spano, and S. J. Schiff, Phys. Rev. Lett. **77**, 4098 (1996).
[43] W. C. Stacey and D. M. Durand, J. Neurophysiol. **83**, 1394 (2000).
[44] D. R. Chialvo, A. Longtin, and J. Müller-Gerking, Phys. Rev. E **55**, 1798 (1997).
[45] M. Rudolph and A. Destexhe, Phys. Rev. Lett. **86**, 3662 (2001).
[46] L. M. Ward, A. Neiman, and F. Moss, Biol. Cybern. **87**, 91 (2002).
[47] M. Stemmler, M. Usher, and E. Niebur, Science **269**, 1877 (1995).
[48] E. Simonotto, M. Riana, C. Seife, M. Roberts, J. Twitty, and F. Moss, Phys. Rev. Lett. **78**, 1186 (1997).
[49] G. Winterer *et al.*, Clin. Neurophysiol. **110**, 1193 (1999).
[50] D. F. Russell, L. A. Wilkens, and F. Moss, Nature (London)

402, 291 (1999).
[51] J. A. Freund, J. Kiernert, L. Schimansky-Geier, B. Beisner, A. Neiman, D. F. Russell, T. Yakusheva, and F. Moss, Phys. Rev. E **63**, 031910-1 (2001).
[52] J. A. Freund *et al.*, J. Theor. Biol. **214**, 71 (2002).
[53] M. T. Huber, H. A. Braun, and J. C. Krieg, Biol. Psychiatry **46**, 256 (1999).
[54] M. T. Huber, H. A. Braun, and J. C. Krieg, Biol. Psychiatry **47**, 634 (2000).
[55] M. T. Huber, H. A. Braun, and J. C. Krieg, Neuropsychopharmacology **28**, S13 (2003).
[56] M. T. Huber and H. A. Braun, Proc. SPIE **5110**, 332 (2003).
[57] N. Ho and A. Destexhe, J. Neurophysiol. **84**, 1488 (2000).
[58] F. S. Chance, L. F. Abbott, and A. D. Reyes, Neuron **35**, 773 (2002).
[59] Y. Shu, A. Hasenstaub, M. Badoual, T. Bal, and D. A. McCormick, J. Neurosci. **23**, 10388 (2003).
[60] J. Wolfart, D. Debay, G. L. Masson, A. Destexhe, and T. Bal, Nat. Neurosci. **8**, 1760 (2005).
[61] A. Longtin, Phys. Rev. E **55**, 868 (1997).
[62] H. C. Tuckwell, *Introduction to Theoretical Neuroscience* (Cambridge University Press, Cambridge, U.K., 1988), Vol. 2.
[63] B. Hille, *Ionic Channels of Excitable Membranes*, 2nd ed. (Sinauer, Sunderland, MA, 1992).
[64] M. T. Huber and H. A. Braun, BioSystems (to be published).
[65] R. F. Fox, I. R. Gatland, R. Roy, and G. Vemuri, Phys. Rev. A **38**, 5938 (1988).
[66] A. Neiman, P. I. Saparin, and L. Stone, Phys. Rev. E **56**, 270 (1997).
[67] H. Gang, T. Ditzinger, C. Z. Ning, and H. Haken, Phys. Rev. Lett. **71**, 807 (1993).
[68] L. Gammaitoni, P. Hanggi, P. Jung, and F. Marchesoni, Rev. Mod. Phys. **70**, 223 (1998).
[69] K. Wiesenfeld and F. Moss, Nature (London) **373**, 33 (1995).
[70] E. Fransen, A. A. Alonso, C. T. Dickson, J. Magistretti, and M. E. Hasselmo, Hippocampus **14**, 368 (2004).